Thermal Comfort and Climatic Potential of Ventilative Cooling in Italian Climates

Giacomo Chiesa, Francesca Fasano, and Paolo Grasso

1 Introduction

Energy consumption for space cooling is characterized by a continuously rising trend [1]. In parallel, the number of installed domestic cooling units is significantly growing, as confirmed by International Energy Agency (IEA) documents and by yearly reports of sector-specific companies [2–4]. The global penetration of the air conditioning market is, in fact, quickly increasing, especially in Asia, but also in the Americas and in Europe [5]. This trend is connected to several causes, including climate change, urban heat islands, comfort culture, and building design choices that are inconsistent with respect to local climate [1, 6]. It is hence evident that alternative solutions for cooling, when environmental conditions are favourable, may be adopted and developed in order to reduce cooling energy needs and consequent GHGs (greenhouse gas emissions) [7]. Among low-energy alternatives, ventilative cooling (VC) is a valuable technique to reduce energy needs and consumption in buildings supporting free-running and/or fan-assisted ventilation for space cooling. This technique was demonstrated to be very effective in reducing overheating risks, but also to guarantee thermal and IAQ (indoor air quality) comfort in buildings during the summer season. However, the ventilative cooling potential occurs when external air temperatures are below comfort thresholds; therefore, its applicability is local and time-specific and is connected to local climate/weather conditions [8, 9]. As underlined for the majority of passive and low-energy cooling solutions, the non-homogeneous specific local potential has limited the current applications of VC with respect to passive heating technologies, that is sunspaces. Nevertheless, a consistent need to support the diffusion of VC solutions is evident, given this approach is not sufficiently covered and valorised by current regulations – see, for

G. Chiesa (✉) · F. Fasano · P. Grasso
Department of Architecture and Design, Politecnico di Torino, Turin, Italy
e-mail: giacomo.chiesa@polito.it

A. Sayigh (ed.), *Achieving Building Comfort by Natural Means*, Innovative Renewable Energy, https://doi.org/10.1007/978-3-031-04714-5_18

example, the recent analysis reported in [10] – even in those climates in which it may support thermal comfort without cooling system activations during the majority of hours [11, 12]. This requires the development of methodologies to calculate the potential of ventilative cooling – see, for example, the results of the IEA EBC ANNEX 62 on Ventilative Cooling and other references [13, 14] supporting the widespread of VC.

1.1 Objectives and Organisation

This chapter aims at investigating, on one hand, climatic key performance indicators (KPIs) for ventilative cooling (VC) (extended summer season from May to September) and, on the other hand, the impact of the same low-energy cooling technology on thermal comfort variations in dynamically simulated building spaces. Additionally, the chapter aims at comparing the two analyses to help define and choose early design indicators to estimate the ventilative cooling potential in terms of thermal comfort and building cooling energy need reduction. The methodology is applied to a large sample of locations, covering the whole Italian territory, to map the thermal comfort/climatic potential of this low-energy dissipation cooling technique.

The chapter is composed of the following sections: Section 2 describes the proposed methodology and introduces the considered KPIs, the assumed reference building, and the climate dataset; Sect. 3 is devoted to reporting the results of the analyses, including climate and comfort KPI distribution at the Italian level. Furthermore, Sect. 3 reports the comparison between the two approaches (the climatic one and the building simulated one); and finally, Sect. 4 reports chapter conclusions.

2 Methodology

As mentioned, the chapter describes, calculates, and compares the climate and comfort/energy effects of VC. This analysis is applied to a sample territory (Italy) to study the local distribution of KPIs. Furthermore, potential correlations between climate-based and building-simulation-based indices are also discussed. The adopted KPIs and their calculation methodology – including the defined simulated sample building and the locations selected for the analysis – are reported in this section. Section 2 is structured in sub-sections that are devoted to defining the assumed key performance indicators (KPIs) considering climate-based analyses (Sect. 2.1) and building-comfort analyses based on dynamic energy simulations (Sect. 2.2). Furthermore, additional sub-sections are included, describing the assumed sample building (Sect. 2.3) and the considered set of locations (Sect. 2.4).

2.1 Climate-Comfort KPIs

Several climate-related KPIs are reported in literature to estimate the local cooling needs and the local potential of ventilative cooling solutions.

Among them, one of the most popular KPIs defining the local climatic cooling needs is the Cooling degree hours/days (CDH/CDD), which was demonstrated to be linearly correlated to the local intensity of building cooling needs – see, for example, [5, 15]. Furthermore, this KPI is also compared to overheating risks during the free-running mode. CDH and CDD integrate hourly differences in temperature between environmental values and a building base temperature over which cooling or overheating is expected. The assumed cooling base temperature may differ according to the purposes of the analysis, ranging from 15.5 °C [16] to 26 °C [17]. Furthermore, the calculation may be assessed for the whole summer period or for specific calculation times. For the purpose of this chapter, the following expression is adopted for the CDH index:

$$\mathrm{CDH} = \sum m_h \cdot \left(\vartheta_{\mathrm{e},h} - \vartheta_{\mathrm{b}}\right) \quad \begin{cases} m_h = 1 \leftarrow \vartheta_{\mathrm{e},h} > \vartheta_{\mathrm{b}} \\ m_h = 0 \leftarrow \vartheta_{\mathrm{e},h} \le \vartheta_{\mathrm{b}} \end{cases} \tag{1}$$

where:

the variable m_h is a climate cooling activation check and ϑ_{b} is the cooling base temperature, ranging for the purpose of this chapter in the domain {18 °C; 21; 24; 26; 28}, while $\vartheta_{\mathrm{e},h}$ is the hourly dry-bulb environmental temperature.

Additional calculation approaches are suggested in literature, such as the approach described in EN ISO 15927-6:2008. European Statistical Office (EUROSTAT), for example, supports the calculation of CDD on the basis of two thresholds and considering daily average temperatures. The first threshold defines for which days the CDD needs to be calculated, while the second, lower one is used as base calculation temperature – see Eq. (2) [18].

$$\mathrm{CDD}_{eu} = \sum m_d \cdot \left(\vartheta_{\mathrm{e},d} - 21\right) \quad \begin{cases} m_d = 1 \leftarrow \vartheta_{\mathrm{e},d} \ge 24°\mathrm{C} \\ m_d = 0 \leftarrow \vartheta_{\mathrm{e},d} < 24°\mathrm{C} \end{cases} \tag{2}$$

where:

$\vartheta_{\mathrm{e},d}$ is the environmental daily average temperature, and 24 °C and 21 °C are the first and second mentioned thresholds, respectively.

Degree days/hours are also at the basis of different KPIs that were developed to climatically analyse the potential impact of low-energy technologies. For example, a series of indices are able to define the residual amount of the CDH ($\mathrm{CDH}_{\mathrm{res}}$, percentage or absolute) by calculating the theoretical impact of different heat gain

dissipation technologies, that is evaporative cooling and ground-coupled earth-to-air exchangers – see, for example [19–21].

Nevertheless, for this work, we calculated the climate cooling potential (CCP) and index that was firstly defined by Artman et al. [22] and supported in several publications, for example [12, 13]. This index is based on the internal-external air temperature difference and is expressed in Kelvin per hour [K/h], suggesting the night cooling potential of ventilative cooling. The calculation methodology is expected to work during night hours (from 19:00 to 7:00), considering an office space conditioned only during the daytime in which internal temperature is following a sinusoidal variation around 24.5 °C of ±2.5 °C (max temperature is set at 19:00). These internal temperature ranges were suggested on the basis of European Committee for Standardization (CEN) thermal comfort categories – for example in EN 16798-4:2019, the comfort category III for offices suggests temperature ranges between 22 and 27 °C in internally conditioned spaces [23]. CCP is generally considered only during night hours to define the night-time mean CCP value in a given period. Hence, the daily average (CCP_d) may be defined by dividing the CCP by the number of days in the considered period. Nevertheless, it is also possible to calculate the cumulative distribution of CCP.

In this chapter, the cumulative CCP is assumed to directly compare results with the cumulative cooling energy savings due to ventilative cooling activation in a conditioned space – see Eq. (3). Nonetheless, this analysis is performed for the whole summer period, considering that ventilative cooling may be also performed during the daytime when external conditions are favourable (controlled ventilation). The CCP_d is also calculated.

$$\mathrm{CCP} = \sum m_h \cdot \left(\vartheta_{\mathrm{b},h} - \vartheta_{\mathrm{e},h}\right) \quad \begin{cases} m_h = 1 \leftarrow \vartheta_{\mathrm{b},h} - \vartheta_{\mathrm{e},h} \geq 2\,^{\circ}\mathrm{C} \\ m_h = 0 \leftarrow \vartheta_{\mathrm{b},h} - \vartheta_{\mathrm{e},h} < 2\,^{\circ}\mathrm{C} \end{cases} \tag{3}$$

where:

$$\vartheta_{\mathrm{b},h} = \left(24.5 + 2.5 \cdot \cos\left(\frac{2\pi\left(h-19\right)}{24}\right)\right)\left[^{\circ}\mathrm{C}\right] \tag{4}$$

and h is the number of daily hours [1–24]. A critical difference in temperature between the base and environmental temperature of 2 °C is assumed, even if higher differences may be considered for a precautionary approach.

In addition to DH-DD indices and based on the same principle, it is possible to define a KPI to calculate the climate heat gain dissipation potential of ventilative cooling. By knowing the airflow rate and the thermal properties of air it is possible to calculate the cooling dissipation Q_{ach} [Wh] by considering the difference in temperature between internal and external air and adopting the well-known expression [9, 24, 25]:

$$Q_{ach} = \sum m_h \cdot ACH \bullet Vol \cdot \rho_{air} \cdot c_{air} \cdot \left(\vartheta_{set} - \vartheta_{e,h}\right) \quad \begin{cases} m_h = 1 \leftarrow \vartheta_{e,h} \leq \left(\vartheta_{set} - 2°C\right) \\ m_h = 0 \leftarrow \vartheta_{e,h} > \left(\vartheta_{set} - 2°C\right) \end{cases} \tag{5}$$

where:

the variable *ACH* is the number of air changes per hour, which is assumed for this paper in the domain {0;2.5;5}; Vol is the assumed net volume [m^3] of the building; air density and heat capacity are assumed to be, respectively, 1.2 [kg/m^3] and 0.28 [W/kg°C], while the set point temperature was set to be equal to the simulated cooling set point (26 °C). Finally, 2 °C was the assumed minimal difference in temperature from the set point, to consider a sufficient activation of ventilative cooling. The latter value generally ranges between 2 and 3 °K – see also the critical temperature description defined in the IEA EBC Annex 62 documents [13].

2.2 Building-Comfort KPIs

Focusing on building thermal comfort indices, two approaches are followed in line with EU standard 16798-1:2019. The first approach refers to mechanically cooled building configurations. In these cases, we assumed the thermal comfort model described in ISO 7730, which is based on the PMV (predicted mean vote) and PPD (predicted percentage of dissatisfied) indices. This approach, in line with the Fanger comfort theory [26, 27], is based on six parameters: four environmental parameters (air temperature, humidity, mean radiant temperature, and relative air velocity) and two personal parameters (metabolic rate and clothing level). Considering statistical correlations based on personal expected thermal sensations, the PMV index classifies user thermal sensation on a 7-point scale, ranging from −3 (very cold) to +3 (very hot), in which values around 0 are the most comfortable (neutral). Different comfort categories are suggested in the EU standard according to PMV ranges around the neutral point – that is category I (±0.2 PMV); II (±0.5 PMV); and III (±0.7 PMV).

The calculation procedure for the PMV and PPD was implemented in line with the one described in both EN and ISO standards by developing a specific Python code. The clothing level is assumed to be 0.7 clo, considering underwear, shirt, trousers, socks, and shoes (ISO 9920) – an intermediate balance between hot central hours of summer and September/May evening – while the metabolic rate was set to 1.2 met, corresponding to standing relaxed or sitting activity conditions – a typical value for residential living spaces (EN 16798-1). In addition to these basic indices, cumulative versions are available. For this study, the cumulative value of PPD whenever hourly PMV is higher than category III is calculated according to the following rule:

$$\mathrm{PPD}_{\mathrm{exceedance}} = \sum m_h \cdot \mathrm{PPD}_h \qquad \begin{cases} m_h = 1 \leftarrow \mathrm{PMV}_h \geq 0.7 \\ m_h = 0 \leftarrow \mathrm{PMV}_h < 0.7 \end{cases} \tag{6}$$

where:

PMV_h is the hourly computed value for predicted mean vote and PPD_h the corresponding hourly predicted percentage of dissatisfied.

The second thermal comfort approach is assumed for free-running building configurations. For the purpose of this work, it is considered that a building is working in a free-running mode in the summer when cooling systems are not present or are turned off. This definition is in line with past and current research projects, that is IEA Annex 62 and H2020 EU-co-funded project E-DYCE [28]. In these cases, the adaptive thermal comfort theory is assumed – see the works of Fergus and Humphreys [29, 30]. The calculation was performed in line with the above-mentioned EN standard, assuming the upper comfort category II as a reference. Additionally, cumulative values of hourly distances from the central comfort line and from upper thresholds of different comfort categories are calculated according to the following rules:

$$\mathrm{dist}_0 = \begin{cases} \sum m_h \cdot \mathrm{dist}_{0,mid,h} & \text{if } 10°\mathrm{C} < \vartheta_{rm,h} < 33°\mathrm{C} \quad \text{where} \quad \begin{cases} m_h = 1 \leftarrow \mathrm{dist}_{0,mid,h} > 0 \\ m_h = 0 \leftarrow \mathrm{dist}_{0,mid,h} \leq 0 \end{cases} \\ \sum m_h \cdot \mathrm{dist}_{0,\mathrm{up},h} & \text{if } \vartheta_{rm,h} \geq 33°\mathrm{C} \quad \text{where} \quad \begin{cases} m_h = 1 \leftarrow \mathrm{dist}_{0,\mathrm{up},h} > 0 \\ m_h = 0 \leftarrow \mathrm{dist}_{0,\mathrm{up},h} \leq 0 \end{cases} \end{cases} \tag{7}$$

$$\mathrm{dist}_3 = \begin{cases} \sum m_h \cdot \mathrm{dist}_{3,mid,h} & \text{if } 10°C < \vartheta_{rm,h} < 33°\mathrm{C} \quad \text{where} \quad \begin{cases} m_h = 1 \leftarrow \mathrm{dist}_{3,mid,h} > 0 \\ m_h = 0 \leftarrow \mathrm{dist}_{3,mid,h} \leq 0 \end{cases} \\ \sum m_h \cdot \mathrm{dist}_{3,\mathrm{up},h} & \text{if } \vartheta_{rm,h} \geq 33°\mathrm{C} \quad \text{where} \quad \begin{cases} m_h = 1 \leftarrow \mathrm{dist}_{3,\mathrm{up},h} > 0 \\ m_h = 0 \leftarrow \mathrm{dist}_{3,\mathrm{up},h} \leq 0 \end{cases} \end{cases} \tag{8}$$

where:

- $\mathrm{dist}_{0,\mathrm{mid},h} = \vartheta_{\mathrm{op,i},h} - (0.33 \cdot \vartheta_{\mathrm{rm},h} + 18.8)$ is the distance from the central comfort line whenever the running mean is in the (10,33) °C range;
- $\mathrm{dist}_{0,\mathrm{up},h} = \vartheta_{\mathrm{op,i},h} - (0.33 \cdot 33 + 18.8)$ is the distance from the central comfort line whenever the running mean is in the [33,x] °C range;
- $\mathrm{dist}_{3,\mathrm{mid},h} = \vartheta_{\mathrm{op,i},h} - (0.33 \cdot \vartheta_{\mathrm{rm},h} + 18.8 + 3)$ is the distance from the upper threshold of comfort category II whenever the running mean is in the (10,33) °C range;

– $dist_{3,\,up,\,h} = \vartheta_{op,\,i,\,h} - (0.33 \cdot 33 + 18.8 + 3)$ is the distance from the upper threshold of comfort category II whenever the running mean is in the [33,x] °C range;

and $\vartheta_{op,\,i,\,h}$ is the hourly indoor operative temperature, while $\vartheta_{rm,\,h}$ is the hourly updated running mean temperature calculated in line with EN 16798-1:2019. Different comfort categories are also considered assuming limits mentioned in the standard.

The cumulative intensity of discomfort for free-running buildings may be adapted to a simpler indicator: the cooling internal degree hours (CIDH). This indicator is the building-correlated counterpart of the CDH indicator – see the definition reported in Pellegrino et al. [31]. For this research, it was calculated as below:

$$\text{CIDH} = \sum m_h \cdot \left(\vartheta_{i,h} - \vartheta_c\right) \quad \begin{cases} m_h = 1 \leftarrow \vartheta_{i,h} > \vartheta_b \\ m_h = 0 \leftarrow \vartheta_{i,h} \le \vartheta_b \end{cases} \tag{9}$$

where:

the variable m_h is the climate cooling activation check and ϑ_c the cooling comfort temperature, assumed in this chapter not only as a fixed reference set point (i.e. 26 °C) but ranging in the domain {18 °C; 20; 22; 24; 26; 28} to verify correlations with climate CDH, while $\vartheta_{i,\,h}$ is the hourly indoor air temperature.

2.3 Building Sample Definition

A sample residential building unit was adopted to test the proposed methodology. The considered unit is a typical flat of a multi-storey building. Its internal organisation and definition are in line with suggested residential building typologies included in well-known architectural technical manuals – see, for example [32, 33] – and in line with the methodological approach followed in previous climate-correlated studies [34]. The considered building is composed of two units per floor, while a single unit is simulated for this chapter. The simulated spaces are considered to be at an intermediate floor with an upper floor and lower floor working at the same

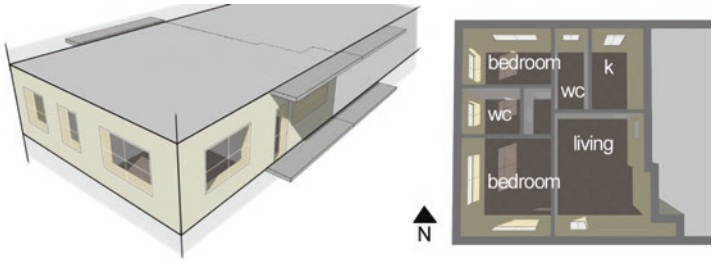

Fig. 1 The considered sample residential building unit

temperature (adiabatic). Similarly, the simulated unit is touching a specular one: Confining walls are also assumed to be adiabatic. Upper-floor balconies are included to consider shading effects – see Fig. 1.

Dynamic hourly energy and thermal simulations are performed by adopting EnergyPlus [35]. Different simulations were performed for each location to compare building scenarios. We investigated, on one hand, the free-running building mode and, on the other hand, the mechanically cooled building mode, assuming EnergyPlus ideal loads and retrieving net energy needs. Five configurations are considered assuming different levels of ventilative cooling air changes per hour (ACH) in order to test the impact of ventilative cooling (VC) – indifferently natural or fan-driven – on cooling energy needs (mechanical cooling mode) and on thermal comfort indices (free-running cooling mode). Table 1 describes the adopted set of simulations.

Ventilative cooling is defined by adopting the scheduled natural ventilation approach in EnergyPlus, supporting VC activation by controlling temperature thresholds. For the free-running mode, external temperature control rules assume that there is no maximum outdoor temperature above which the ventilation is shut-off since there is no other cooling system in the building, although an activation difference in temperature between internal and external values of 2 °C is defined in line with climate KPIs described above. Differently, for the mechanical cooling mode, a control on maximum outdoor temperature (26 °C) is also added to avoid the risk to introduce external airflows in the building at a temperature higher than the cooling set point, which is set to 26 °C, with a consequent rise of cooling loads. Cooling scheduling is activated, when control conditions are appropriate, for the whole extended summer period. Internal gains and occupancy profiles are assumed in line with the ones suggested by EnergyPlus references – see also the description in [34]. Envelope definition is the same in both free-running and mechanically cooled modes. The U-value of walls was set to 0.287 [W/m^{2}K] (10 cm of insulation), while the U-value for windows was 1.499 [W/m^{2}K] (Double glass, Low-E with argon). Simulations are controlled by using Python coding.

Table 1 The adopted simulation configurations (VC = ventilative cooling)

Free-running mode	ACH	Mechanical-cooling mode	ACH
1a. Reference case	0	1b. Reference case	0
2a. low VC	2.5	2b. low VC	2.5
3a. VC	5.0	3b. VC	5.0

2.4 Climate Data and Locations

For this chapter, the above-described KPIs are applied to the whole Italian territory, assuming a calculation point for each municipality. The Italian municipality database was based on the ISTAT (national statistics agency) data (31/12/2017 version) and includes 7978 data points.

Typical meteorological years (TMY) for each point are retrieved by the Meteonorm tool [36] assuming reference periods 1991–2010 and 2000–09 for irradiation and for temperatures, respectively. For all locations, the entire set of simulations was performed, including the calculation of simulated and climate-related KPIs. This large dataset (47,868 simulations) allows comparison analyses among different KPIs. A comparison between building comfort-related indices and external-climatic KPIs is performed to verify the possibility to predict the ventilative cooling potential on building comfort and energy needs without running dynamic building energy simulations.

The analysis is performed for an extended summer period ranging from May to September (included). This assumption will allow us to better evaluate the ventilative cooling potential to cover the summer overheating also in the hottest locations, in which a reduced summer period (e.g. June to August) will not be representative of the whole summer season. This assumption is in line with previous analyses [20].

KPI devoted maps are produced by using a geospatial Python plotting library, while the Italian borders are retrieved by a GeoJSON file provided by Openpolis [37].

3 Results

Three main categories of results are presented. On one hand, KPI results – both climatic (Sect. 3.1) and building-related ones (Sect. 3.2) – are illustrated. On the other hand, mutual correlations between climate and simulated building KPIs are analysed (Sect. 3.3) to verify consistencies and the ability of climate indices to represent preliminary building trends.

3.1 Climate-Based KPIs

The distribution of climatic KPIs over the Italian territory is illustrated, with the aim to represent local specific behaviours.

In line with the description in Sect. 2, the CDH indicator represents the cumulative hourly differences between the environmental air temperature and an assumed base reference temperature, while CDD considers a daily cumulative cooling severity. Figure 2a shows the CDH distribution for the whole dataset, considering 18 °C as base temperature, while Fig. 2b illustrates the CDD distribution. Both KPIs

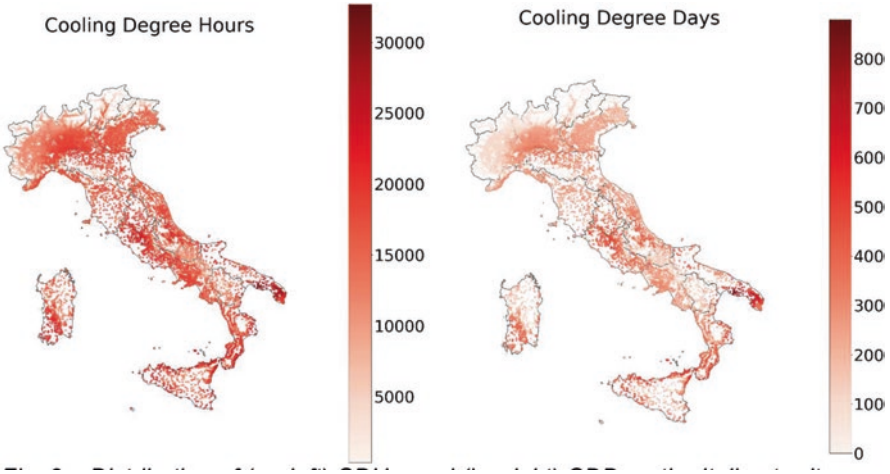

Fig. 2 Distribution of (**a** – left) CDH_{18} and (**b** – right) CDD on the Italian territory

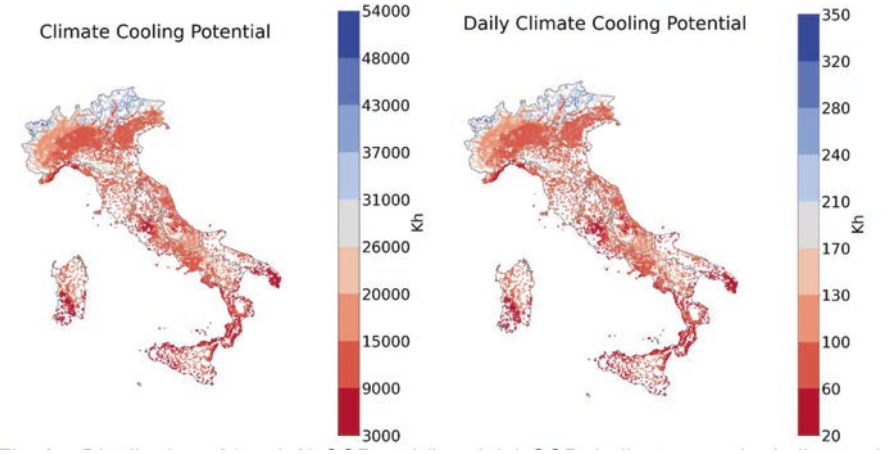

Fig. 3 Distribution of (**a** – left) CCP and (**b** – right) CCP_d indicators on the Italian territory

largely depend on the specific local climate conditions. In the northern mountain zones, lower values of both CDH and CDD are retrieved, given the number of overheating hours or days is very limited. Only for a few hours, the TMY environmental temperatures are above the assumed thresholds, while in the central and southern areas these KPIs reached higher values due to the warmer climate conditions. It could be interesting to notice that locations nearer to Rome and Milan, which are the two most populated Italian cities – see ISTAT databases [38], show higher CDH and CDD values. This phenomenon is in line with the expected impact of urban heat island conditions. In these sites, higher cooling needs or higher discomfort conditions are expected. Furthermore, the high concentration of building units underlines

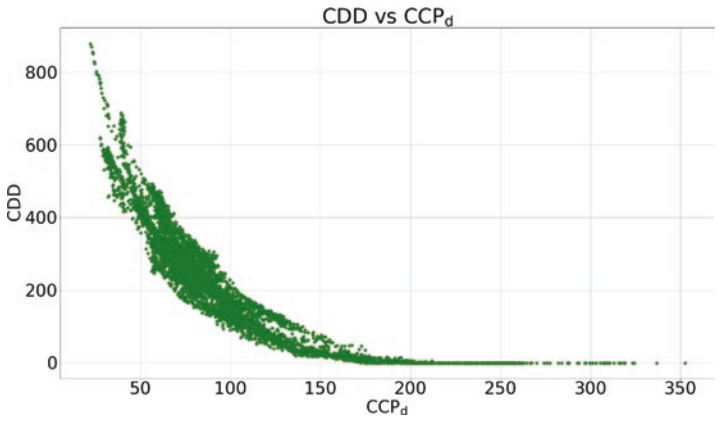

Fig. 4 CCD vs. CCP_d comparison

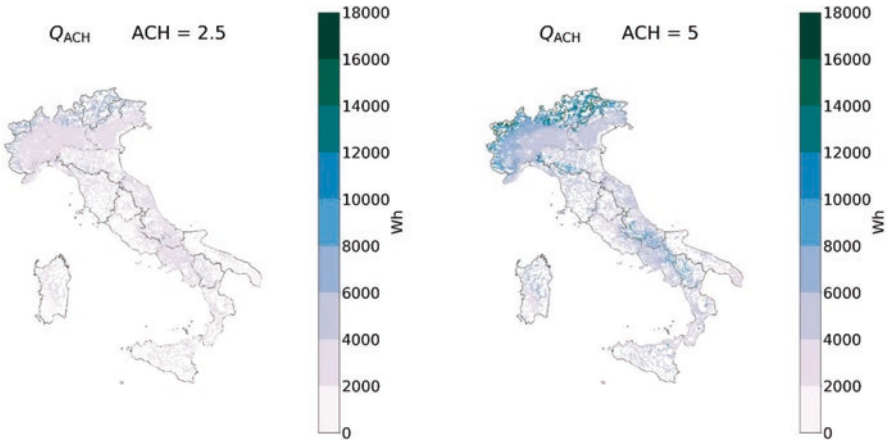

Fig. 5 Distribution of Q_{ACH} indicator on the Italian territory

that the adoption of low-energy cooling technologies in these locations may have an impact on a high number of end-users.

Focusing on the climate ventilative cooling KPIs, Fig. 3 reports the Italian distribution of (a) CCP and (b) CCPd values. These two maps show that the zones in Italy with the higher climate cooling potential are located in the north of the peninsula, due to the colder climate, which allows a higher natural dissipative cooling potential by adopting air as a heat sink. For most summer hours, the environmental air temperature in such zones is low enough to provide climate comfort conditions. Instead, the southern Italian locations are affected by lower ventilative cooling potentials due to higher external temperatures. This condition limits in both time and intensity the possibility to adopt ventilative passive cooling methodologies to achieve a climatic indoor comfort when internal temperatures rise above the comfort threshold.

Figure 4 underlines that CDD is correlated with CCP_d by following a decreasing exponential trend. In fact, a high CDD means that the cooling-correlated energy demand of a virtual building is high when the daily external temperature is above the assumed base threshold, prompting people to turn on mechanical cooling systems when present. Nevertheless, CCP_d values retrieved for hotter days are also expected to be low, since the high environmental air temperature limits the applicability of ventilative cooling. Oppositely, a higher climate cooling potential for a specific day means that, at least at night, environmental temperatures are lower, allowing ventilative cooling activations and consequently a lower virtual climatic cooling demand.

Figure 5 shows the cooling dissipation potential (Q_{ach}) – see Eq. (5) – for the two assumed ACH values. The ACH values in climate analyses are based on the assumed sample building volume to allow KPI comparison. The analysis shows that with an ACH equal to 2.5, the cooling dissipation potential by ventilative cooling is limited in most locations. Differently, considering an ACH equal to 5, several Italian zones – in particular the mountain ones in the north and the one at the centre of the Peninsula – are characterized by an evident natural ventilation dissipative potential able to virtually reduce space cooling needs.

Furthermore, Fig. 6 compares the two calculated climatic ventilative cooling potential KPIs. This figure shows that Q_{ach} and CCP_d are almost linearly correlated. The CCPd may in fact be translated to a dissipation potential by considering an airflow – see, for example, [39]. Although, this result underlines that both indices may be adopted to describe the ventilative cooling potential of a location, even if Q_{ach} is directly reflecting the dissipative potential for a given ACH, while CCP_d focuses on climate ventilative cooling availability.

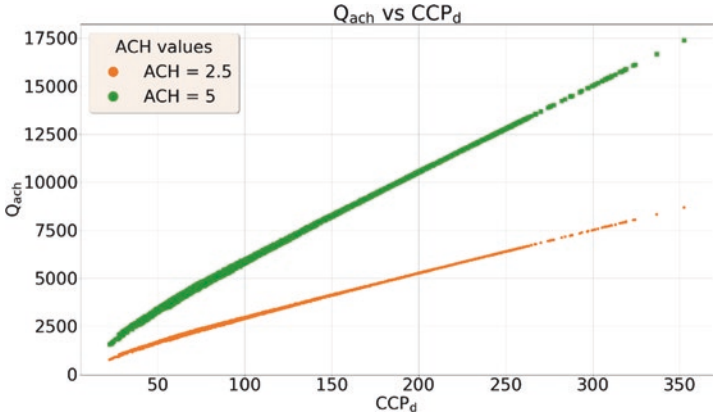

Fig. 6 Q_{ach} vs. CCP_d comparison

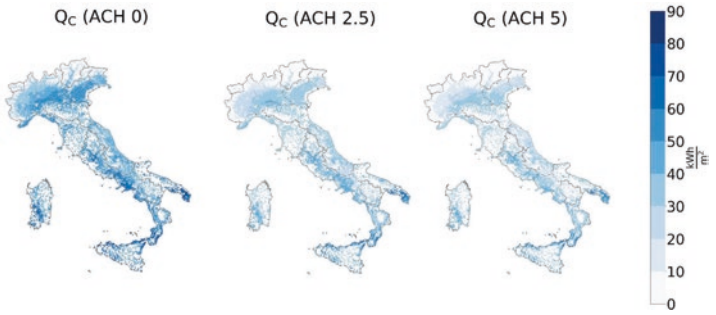

Fig. 7 Building simulation results under mechanical cooling mode. Cooling need distribution in the Italian territory (**a**) without ventilative cooling and with ventilative cooling at different ACH – (**b**) 2.5 and (**c**) 5

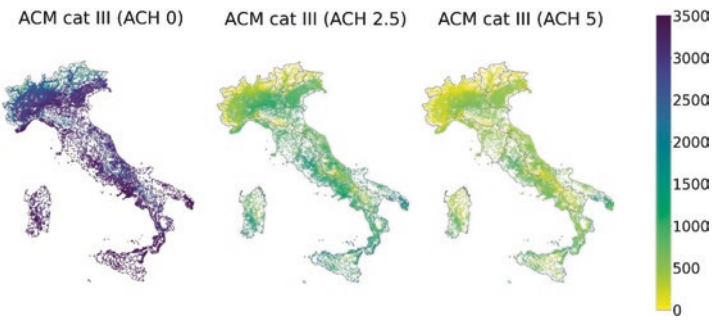

Fig. 8 No. of hours over ACM Cat. II for (**a**) the case without ventilative cooling, (**b**) with a ventilative cooling ACH of 2.5, and (**c**) an ACH of 5

3.2 Building-Based Comfort KPIs

Section 3.2 reports the building simulation results focusing on both mechanical-cooling mode and free-running building mode. Considering the mechanical-cooling mode, Fig. 7 shows that cooling needs in Italy are correlated to different climate conditions – see Fig. 7a. This location-dependent distribution of cooling needs is even more evident when ventilative cooling is considered – see Fig. 7b, c. Nevertheless, the adoption of ventilative cooling strategies can drastically reduce the cooling needs in the majority of locations of the Peninsula. In several cases, ventilative cooling is more than halving the local energy cooling need. The difference between the case with an ACH of 2.5 and the one with an ACH of 5 is not as large as the difference between ACH 2.5 and no ACH, suggesting that even with limited airflow rates, ventilative cooling may strongly reduce building cooling needs in Italy.

Focusing on the free-running mode, Fig. 8 shows the distribution of the number of discomfort hours (above adaptive comfort mode – ACM – upper category II)

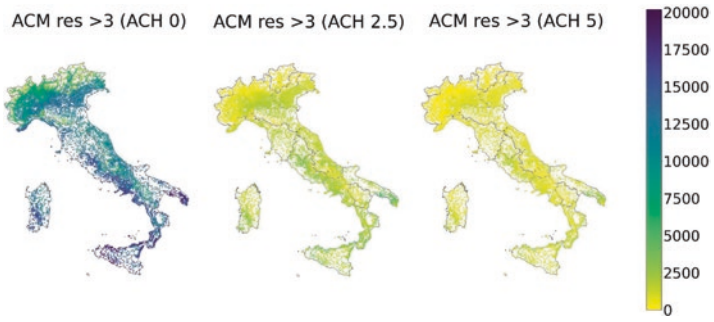

Fig. 9 Cumulative distances from ACM Cat. II upper threshold, varying ventilation ACH

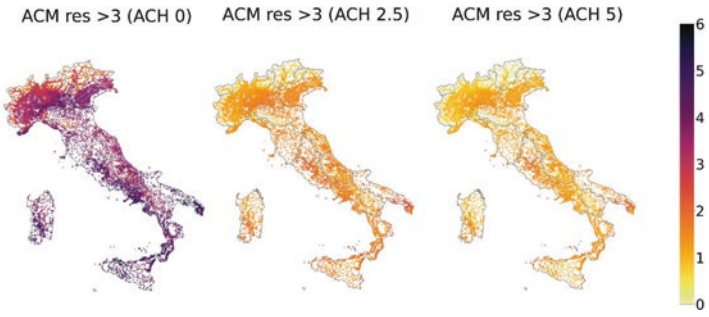

Fig. 10 Average distances from ACM Cat. III lower threshold, varying ventilation ACH

under different ACHs – (a) without ventilative cooling; (b) with ACH set to 2.5; and (c) with an ACH of 5. These maps clearly underline that ventilative cooling may strongly reduce the number of discomfort hours in free-running buildings in almost all Italian locations. In this building mode, a difference between ACH values is underlined especially in southern coastal locations and in the Po Valley. Residual discomfort hours are evident even with a higher ACH in the Eastern part of Apulia regions and in some Tyrrhenian sites, which are also the ones that show higher residual cooling needs in the mechanical cooling mode.

To consider not only the time distribution of discomfort hours but also the discomfort intensity, Fig. 9 reports the cumulative distance from the adaptive comfort model category II upper limit. Comfort category II is assumed considering general suggestions for residential spatial units, assuming in this analysis that discomfort is composed of hours in which building simulated conditions are in both summer Cat. III and Cat. IV – see EN 16798-1. This figure is, on one hand, confirming the above results, while, on the other hand, it shows that even in those locations in which residual discomfort hours are underlined, the intensity of the discomfort may be drastically reduced by adopting ventilative cooling solutions.

Figure 10 shows the same results reported in Fig. 9, but averaged on the basis of the number of discomfort hours shown in Fig. 8. These specific maps are useful to

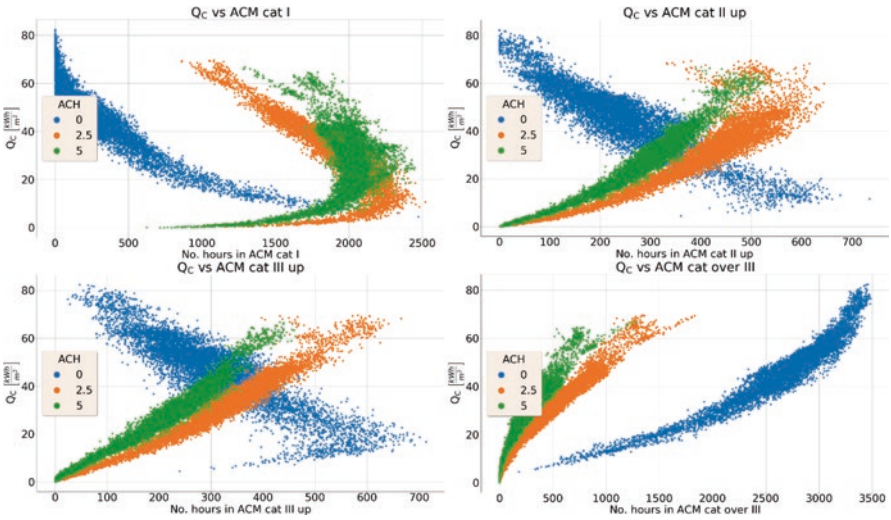

Fig. 11 Cooling consumption (simulated cases B – see Table 1) vs. No. of hours in ACM category (**a**) I, (**b**) II, (**c**) III, and (**d**) IV (simulated cases A – see Table 1) considering different ACHs

give consistency to the discomfort intensity expressed in Kelvin per hour, a synthetic value able to clearly represent discomfort consistency. The aforementioned ability of ventilative cooling to reduce discomfort is immediately evident here, the discomfort intensity shifting in the hottest locations from about 5 [K/h] to about 2 [K/h], a more tolerable value, very near to the upper comfort boundary of adaptive comfort category III (moderate expectations). The distance between the upper limit of Cat. II and III is in fact 1 °C.

Furthermore, a series of correlation analyses have been performed by plotting the cooling energy needs of buildings under mechanical cooling mode as a function of the number of hours for different adaptive comfort categories, considering the simulation results of buildings under free-running cooling mode with the same ACH – see Table 1. These graphs are useful to underline potential virtual correlations between cooling needs and free-running discomfort values. Figure 11 shows the cooling needs of mechanically cooled cases in relation to the number of free-running hours recorded in (a) adaptive comfort category I, (b) Cat. II, (c) Cat. III, and (d) Cat. IV, where the latter includes all discomfort hours outside the moderate comfort category, and the others encompassing, respectively, the hours below the Cat. I upper limit, between Cat. I and Cat. II upper limits, and the hours between Cat. II and III upper limits to avoid hour repetitions (theoretically, Cat. II also includes all hours in Cat. I). These graphs illustrate that in the first three cases – the ones representing different comfort expectations – there is an inverse relationship (ACH = 0) between the number of hours in the comfort category (free-running mode) and cooling needs (mechanical-cooling mode). Other than the last category (discomfort for all expectation levels), a direct correlation is shown for all ACHs, although when VC is considered, a reduction in hours in this category is strongly underlined in all

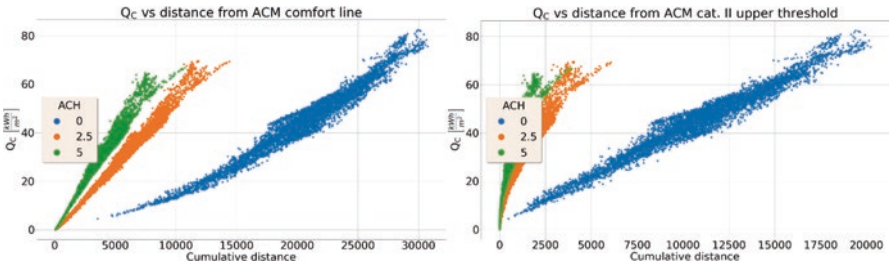

Fig. 12 Cooling consumption (simulated cases B – see Table 1) vs. the cumulative distance from the adaptive thermal comfort (**a**) running mean temperature and (**b**) upper limit of category II (simulated cases A – see Table 1) considering different ACHs

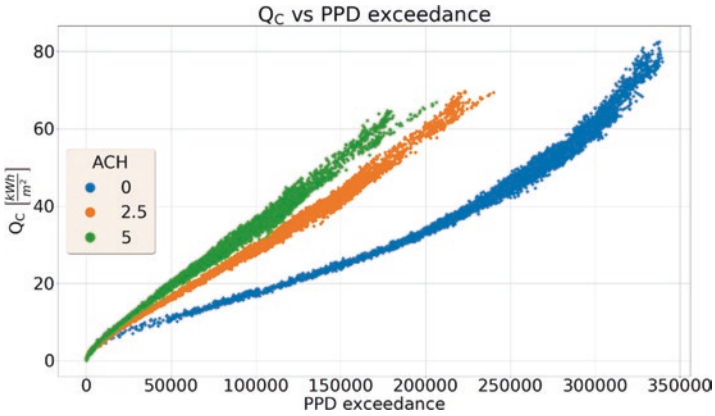

Fig. 13 Cooling consumption (mechanical-cooling mode) vs. PPD exceedance (free-running cooling mode), varying ACH

cases – as mentioned in the previous analyses. ACH activation is impacting the number of hours moving from higher to lower adaptive comfort categories. The difference between ACH activated and ACH = 0 cases is linked to the fact that mechanical cooling works on a fixed set point (26 °C) while adaptive comfort does not. For this reason, hours turned to comfort by ventilative cooling in free-running mode have a corresponding mechanical cooling need for the same ACH value, and the higher the comfort category, the higher the slope of the regression line of VC cases – see, especially, the change among Fig. 11b–d. Nevertheless, it is expected that this outcome will be more evident when discomfort intensity is assumed instead of comfort hours, while direct correlations will be underlined for all cases.

Figure 12 plots the simulated building energy needs as a function of the adaptive comfort cumulative distance from (a) the running mean temperature and (b) the upper limits of comfort Cat. II considering free-running corresponding cases. These graphs show that a correlation is evident between the two building functioning modes. The envisaged slope of regression lines is higher when ACH is active. A

slight difference is underlined for ACH 5 with respect to 2.5, but a very evident benefit is retrieved between ventilated cases with respect to the reference case (ACH = 0) supporting the high potential of VC in the Italian territory.

Additionally, cooling needs are compared to the PPD exceedance calculated for the corresponding free-running building cases. This analysis is forcing the above results when Fanger-correlated comfort indices are assumed – which is a VC non-favourable model. Figure 13 shows that cooling needs and free-running PPD exceedance define evident correlation paths for all ACH cases. Hence, the positive impact of VC is underlined even when the adaptive comfort model is not assumed.

3.3 Comparisons Between Climate and Building KPIs

In this section, the results of Sects. 3.1 and 3.2 are compared. Firstly, the building energy need is compared to the climate CDH and CDD. Figure 14 shows the comparison regression lines for (a) Qc vs. CDH considering different CDH base temperatures, and (b) Qc vs. CDD. In all cases, the three levels of ACH are also plotted. A clear correlation between climate and building indices is underlined and the regression model confidence is growing at higher ACHs, given that in these cases the extra effects of building gains are reduced by dissipation. Table 2 reports the retrieved coefficients of determinations (R^2) for different polynomial degrees for the CDH case considering the different base temperatures. In line with other works [34], lower base temperatures better represent, as climate KPIs, the correlated building cooling energy need, especially when VC is not activated. This outcome is directly correlated to the meaning of base temperature in the summer, cooling needs in a building being connected not only to external air temperature, but also to solar and internal gains. Hence, the adoption of a CDH_{18} (or lower) is suggested when this climate KPI is used to climatically analyse the local energy needs. Similarly, Table 3

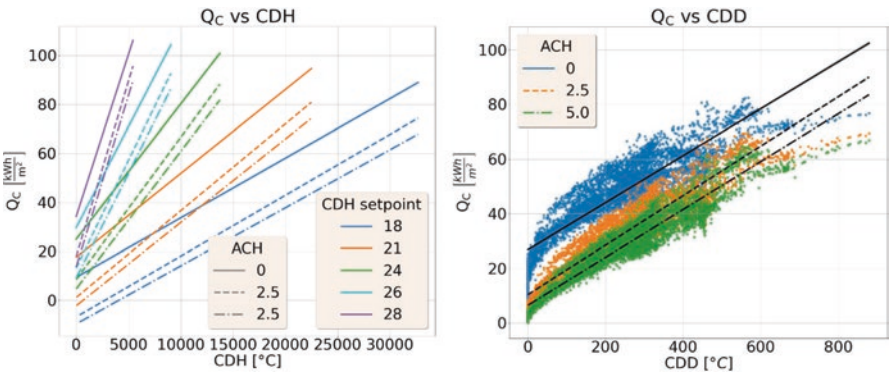

Fig. 14 Building cooling energy needs vs. (**a**) CDH – for different base temperatures, and (**b**) CDD considering different ACH values

Table 2 R^2 results of Qc vs. CDH for different base temperatures – see also Fig. 14a

	Base = 18 ° C	21 ° C	24 ° C	26 ° C	28 ° C
ACH = 0.0	0.893	0.844	0.749	0.656	0.537
ACH = 2.5	0.930	0.904	0.828	0.745	0.629
ACH = 5.0	0.930	0.915	0.850	0.772	0.661

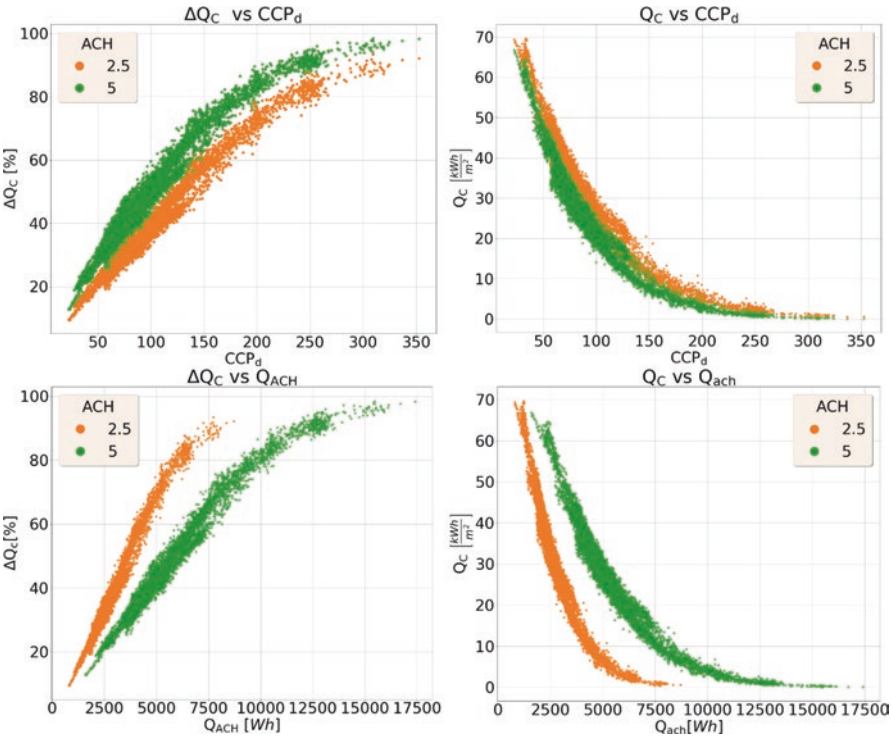

Fig. 15 The difference (percentage of the reference case) in building cooling needs between the reference case (ACH = 0) and the other ACH cases vs. (**a**) CCP_d and (**c**) Q_{ach}. Building cooling energy needs vs. (**b**) CCP_d and (**d**) Q_{ach} considering different ACH values for cooling needs

Table 3 R^2 results of Qc vs. CDD analysis – see also Fig. 14b

	Polynomial degree 1	Polynomial degree 2	Polynomial degree 3
ACH = 0.0	0.805	0.850	0.862
ACH = 2.5	0.893	0.912	0.916
ACH = 5.0	0.918	0.929	0.930

shows R^2 values for the regression lines of the case reported in Fig. 14b. The retrieved values, performed for different polynomial degrees, show that CDD also has a very good potential in representing (climatically) the building cooling energy needs. Even in this case, higher ACHs will increase the correlation. Nevertheless,

the CDH_{18} looks to have a slightly higher correlation potential being based on hourly values as opposed to average daily ones.

Furthermore, the other considered climate KPIs are compared with the building simulation results. Figures 15a, b show the difference in building cooling needs between the reference case (ACH=0) and the other ACH configurations (mechanical cooling mode), respectively, expressed as a percentage of the reference case and plotted as a function of the climate CCP_d indicator. Graph (b) underlines that CCP_d and building cooling needs are strongly inversely correlated and that when an ACH of 5 is assumed for the VC building configuration, a slightly higher dissipative potential is shown. The percentage of coverage of the original building cooling needs with VC – see Fig. 15b – ranges from 9.5% to 93.5% for an ACH of 2.5 and from about 12.9% to 98.5% for an ACH of 5.

A similar result is also shown for the Q_{ach} indicator. Figures 15c, d report the same analyses for the latter KPI. Unlike CCP_d, Q_{ach} better represents differences between ACH values since it includes the airflow in its calculation process, while the other indicator is only based on cumulative temperature differences. Nevertheless, both may be adopted to predict, since early design (climate analyses), the local VC potential.

Climate vs. building analyses are also performed by comparing climate indices and the adaptive thermal discomfort defined for building cases in the free-running mode. Firstly, following the same approach as above, CDD, CDH_{18}, and CDH_{26} are compared with the cumulative intensity of adaptive discomfort. Two reference limits are assumed: a theoretical distance from the running mean temperature – here called ">0" – also including comfort conditions until upper Cat. I, but able to represent all cases; and distances from the upper limit of comfort Cat. II (positive values only). Tables 4 and 5 report the R^2 values of polynomial regression lines plotting the adaptive comfort cumulative discomforts as a function of the local CDD and CDH (both CDH_{18} and CDH_{26}), respectively. For higher polynomial degrees, a slightly higher coefficient of determination is reached in both cases, even if these differences are very limited, especially when buildings are set at a high ACH value, that is 5. Similarly, Fig. 16 shows the same behaviour described above by using a graphical representation. As underlined in both tables, the case without VC (ACH = 0) is highly statistically dispersed, while stronger correlations are underlined in VC cases. Both indices are able to represent the expected discomfort intensity in the free-running building mode. Also in this case, a low CDH base temperature (18 °C) shows a higher correlation with respect to adaptive cumulative discomfort values when compared to a higher CDH base temperature (26 °C).

Table 4 R^2 results (adaptive cumulative discomfort vs. CDD)

	Polynomial degree 1		Polynomial degree 2		Polynomial degree 3	
	>0	>3	>0	>3	>0	>3
ACH = 0.0	0.711	0.734	0.765	0.768	0.787	0.783
ACH = 2.5	0.916	0.930	0.926	0.940	0.930	0.940
ACH = 5.0	0.961	0.926	0.961	0.968	0.963	0.968

Table 5 R^2 results (adaptive cumulative discomfort vs. CDH)

	Polynomial degree 1		Polynomial degree 2		Polynomial degree 3	
	>0	>3	>0	>3	>0	>3
	CDH_{18}					
ACH = 0.0	0.811	0.805	0.822	0.806	0.825	0.807
ACH = 2.5	0.932	0.852	0.940	0.942	0.940	0.943
ACH = 5.0	0.934	0.803	0.967	0.962	0.967	0.965
	CDH_{26}					
ACH = 0.0	0.567	0.584	0.647	0.645	0.693	0.679
ACH = 2.5	0.790	0.848	0.823	0.848	0.838	0.850
ACH = 5.0	0.857	0.883	0.869	0.894	0.877	0.895

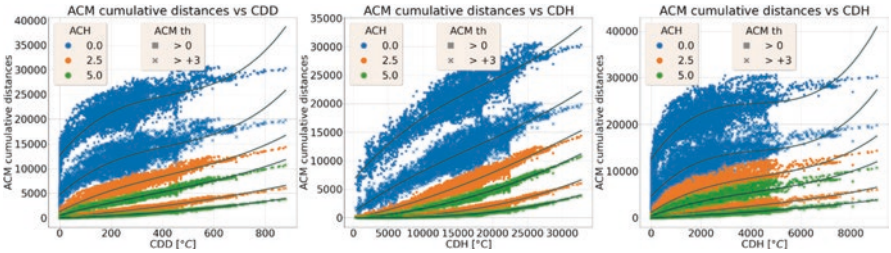

Fig. 16 Building free-running mode. Adaptive thermal comfort cumulative distances from the running mean temperature and upper limit of Cat. II vs. (**a**) CDD, (**b**) CDH_{18}, and (**c**) CDH_{26}

Furthermore, CCP (cumulative) values are compared to adaptive thermal comfort hours in free-running building mode considering the effect of VC. This comparison is based on changes due to VC in the number of hours for comfort categories with respect to the hour distribution of the reference case (ACH = 0). Figure 17a plots the number of hours for different adaptive comfort categories as a function of the local CCP when ACH=0. This figure underlines that, at low CCP values, a high number of hours are included in Cat. IV, while a higher number of hours in Cat. I is underlined for higher CCP values. Differently, the other graphs in Fig. 17 show differences in the number of hours for each category between the reference case and the VC ones. Figure 17b shows an almost linear correlation between the increase (negative delta) in hours below the comfort Cat. I and local CCP values when VC is considered. Focusing on Cat. I, Fig. 17c underlines that at low CCP, an increase in hours in this category is underlined for VC cases, while a reduction in the original hours in this range is shown at a higher CCP, suggesting that VC is moving them below the lower limit. The same trend is evident in all the following graphs, which show that VC is supporting a reduction in space temperatures with respect to the reference case (ACH = 0), especially for locations with a high CCP. Nevertheless, Fig. 17f shows that a reduction in hours above the upper limit of Cat. III is evident for all sites.

Considering the other VC climate indicator, a strict inverse proportionality is underlined in Fig. 18 between local Q_{ach} and the corresponding cumulative distance

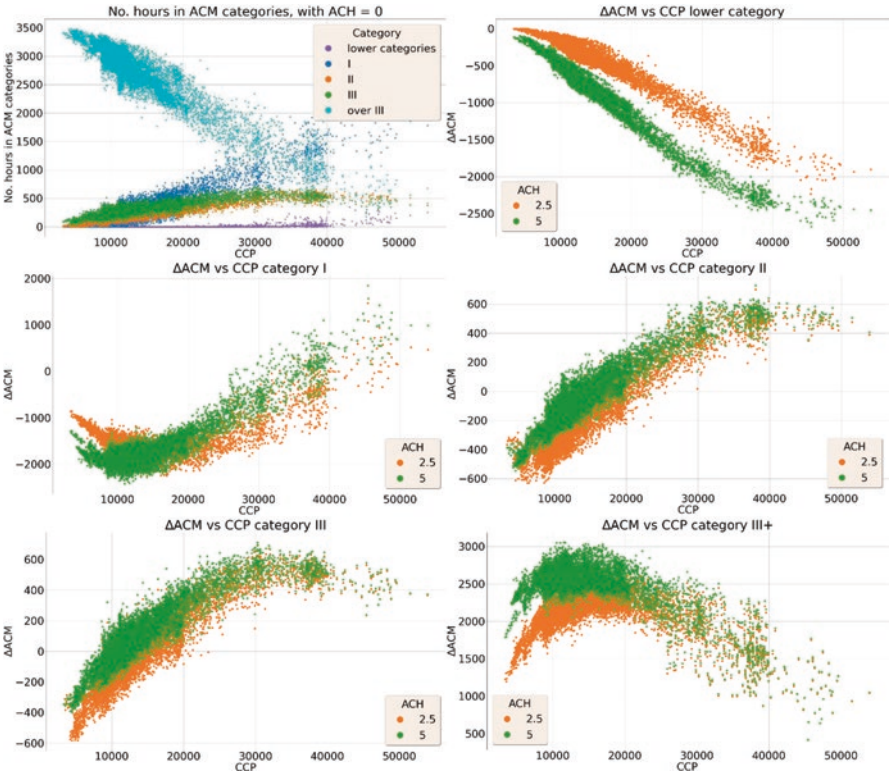

Fig. 17 Free-running building hours for adaptive comfort categories vs. CCP, considering (**a**) the simple number of hours in the reference case with ACH = 0; differences in the number of hours (case ACH_0 – case $ACH_{2.5}$ and ACH_5) by adaptive comfort category: (**a**) below the lower limit of Cat. I; (**c**) in Cat. I; (**d**) in Cat. II; (**e**) in Cat. III; and (**f**) above the upper limit of Cat. III

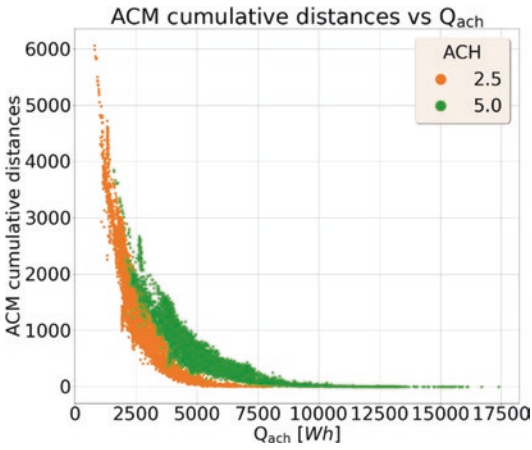

Fig. 18 Building adaptive comfort cumulative distances from the upper limit of Cat. II plotted as a function of the local Q_{ach}

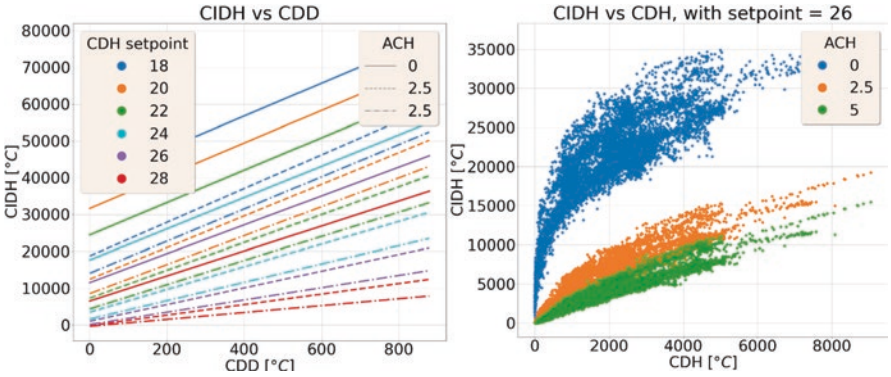

Fig. 19 Building CIDH plotted as a function of local (**a**) CDD and (**b**) CDH. In (**a**), different CIDH base temperatures are assumed, while in (**b**), both KPIs have a base temperature of 26 °C

Table 6 R^2 results ($CIDH_{base}$ vs. CDD)

	Base = 18 ° C	20 ° C	22 ° C	24 ° C	26 ° C	28 ° C
ACH = 0.0	0.778	0.779	0.787	0.801	0.820	0.843
ACH = 2.5	0.851	0.873	0.904	0.940	0.970	0.971
ACH = 5.0	0.878	0.907	0.943	0.974	0.987	0.961

from the adaptive thermal comfort upper limit of Cat. II (considering only the hours above this limit). A higher ACH value, that is 5 instead of 2.5, increases the local VC potential.

Finally, for the free-running building cooling mode, the CIDH is also assumed, considering that in mechanical cooling mode this indicator is functional to the selected set point temperature, thus losing relevance. Figure 19 compares local climate (a) CDD and (b) CDH vs. building CIDH. In graph (a), different CIDH base temperatures are compared with CDD, showing good correlations especially for higher bases – see Table 6. Differently, in graph (b), $CIDH_{26}$ is compared to the corresponding environmental CDH_{26} for different ACH values. High R^2 values are retrieved, as shown in Table 7.

A deeper analysis was performed by comparing the coefficient of determinations for different CDH and CIDH base temperatures (free-running building mode). Results are plotted in Fig. 20a–c for the three considered ACH values {0;2.5;5}, respectively. As mentioned above, a very high correlation is underlined in all cases, especially for CDH_{18}, in line with the results of the mechanical-cooling building mode. For lower CDH bases, medium-to-high CIDH temperatures show a higher R^2, while by increasing the ACH the optimal combination moves to lower CIDH base temperatures. This latter result is due to the increase in the correlation between indoor and environmental conditions, thanks to greater airflow exchanges.

Table 7 R^2 results (CIDH vs. CDH – base temperature 26 for both)

	Polynomial degree 1	Polynomial degree 2	Polynomial degree 3
ACH = 0.0	0.820	0.866	0.883
ACH = 2.5	0.970	0.972	0.973
ACH = 5.0	0.987	0.988	0.988

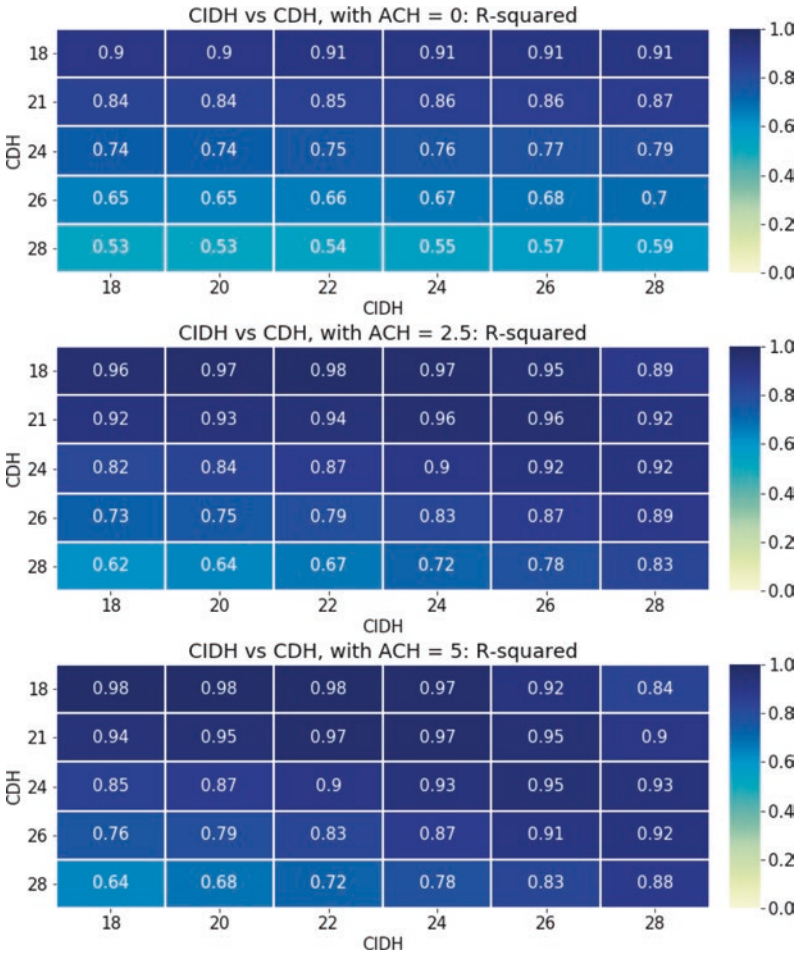

Fig. 20 R^2 values combining different ACH and CIDH base temperatures for: (**a**) ACH = 0; (**b**) ACH = 2.5; and (**c**) ACH = 5 in free-running building mode

4 Conclusions

The chapter analyses the ventilative cooling potential in Italy by performing climate-based and dynamic building energy simulation analyses. The research defines a

series of KPIs, both climate and building-simulation based, to represent VC potentialities. A correlation is underlined between climate and building-simulation retrieved KPIs. This supports the possibility to analyse, since the early design stages, such as building programming – that is when a specific building shape is not yet finalized – the VC potential of a location and the local need for cooling in terms of climate intensity. This possibility is very important to support, in the earliest stage possible, the identification of correct bioclimatic and low-energy solutions to reduce space cooling energy needs and take advantage of the local natural/low-energy cooling heat sink potential.

Additionally, the chapter underlines a direct correlation between mechanically cooled building indicators and free-running building ones, which is an important outcome toward the possibility to correlate the performances of these two types of cooling approaches considering potential evaluations and optimisations, for example for advanced control modes or to define the urgency of cooling system installation.

Finally, results have shown that in almost all Italian locations VC may considerably reduce cooling energy needs when coupled with mechanically cooled spaces and turn a large number of discomfort hours to comfort hours in free-running buildings.

Considering the limitations of this study, the presented work is based on a single TMY database, while in another ongoing research, a larger set of climate databases will be considered including past, present, and future TMY models to verify the consistency of the VC potential under climate changes and under specific perturbation phenomena, such as heatwaves. Additionally, in this study, building data is based on the simulation of a single residential model, while in the future, this analysis is expected to be expanded considering different building configurations, for example referencing the Typology Approach for Building Stock Energy Assessment (TABULA) building database and different envelope parameters. Finally, these indicators will be compared in real building operational conditions to verify the obtained results.

Acknowledgements This work includes preliminary results by WP3 (T3.2) of the PRELUDE project [40] that has received funding from the European Union Horizon 2020 research and innovation programme under Grant Agreement N°958345.

References

1. M. Santamouris, ed., Advances in Passive Cooling, Earthscan, London, 2007.
2. Daikin Industries, Annual Report 2019. Fiscal Year Ended March 31, 2019, 2019. https://www.daikin.com/investor/data/report/daikin_jar19.pdf.
3. The Future of Cooling – Analysis, IEA. (n.d.). https://www.iea.org/reports/the-future-of-cooling (accessed June 4, 2020).
4. IEA Electricity Information 2020, (n.d.). http://wds.iea.org/wds/pdf/ele_documentation.pdf.

5. M. Santamouris, ed., Cooling energy solutions for buildings and cities, World Scientific, New Jersey, 2019.
6. G. Chiesa, M. Grosso, D. Pearlmutter, S. Ray, Editorial. Advances in adaptive comfort modelling and passive/hybrid cooling of buildings, Energy and Buildings. 148 (2017) 211–217.
7. P. Holzer, T. Psomas, eds., Ventilative cooling sourcebook, IEA EBC Annex 62, Aalborg University, Aalborg, 2018.
8. B. Givoni, Man, climate, and architecture, Elsevier, Amsterdam, New York, 1969.
9. M. Grosso, ed., Il raffrescamento passivo degli edifici, IV, Maggioli, Sant'Arcangelo di Romagna, 2017.
10. C. Plesner, M.Z. Pomianowski, Ventilative Cooling in Standards, Legislation and Compliance tools, in: Innovations in Ventilative Cooling, SPRINGER, Cham, 2021: p. 26pp.
11. F. Flourentzou, J. Bonvin, COOLINGVENT – Refroidissement par ventilation pour les bâtiments à basse consommation, rénovés ou neufs. IEA ECBCS Annex 62 on Ventilative cooling, OFEN, Geneva, Switzerland, 2017.
12. G. Chiesa, M. Kolokotroni, P. Heiselberg, eds., INNOVATIONS IN VENTILATIVE COOLING., SPRINGER, S.l., 2021.
13. M. Kolokotroni, P. Heiselberg, IEA EBC Annex 62 – Ventilative Cooling State-of-the-Art Review, Aalborg University, Aalborg, 2015. https://venticool.eu/wp-content/uploads/2013/09/SOTAR-Annex-62-FINAL.pdf.
14. P. Heiselberg, IEA EBC Annex 62 – Ventilative Cooling Design Guide, Aalborg University, Aalborg, 2018.
15. M. Santamouris, D. Asimakopolous, eds., Passive Cooling of Buildings, James and James, London, 1996.
16. CISBE, Degree-days: Theory and application, The Chartered Institution of Building Services Engineers, London, 2006.
17. H. Xuan, B. Ford, Climatic applicability of downdraught cooling in China, Architect. Sci. Rev. 55 (2012) 273–286.
18. EUROSTAT, Energy statistics – cooling and heating degree days (nrg_chdd), (2019). https://ec.europa.eu/eurostat/cache/metadata/en/nrg_chdd_esms.htm.
19. G. Chiesa, Calculating the geo-climatic potential of different low-energy cooling techniques, Build. Simul. 12 (2019) 157–168. https://doi.org/10.1007/s12273-018-0481-5.
20. G. Chiesa, N. Huberman, D. Pearlmutter, Geo-climatic potential of direct evaporative cooling in the Mediterranean Region: a comparison of key performance indicators, Building and Environment. 151 (2019) 318–337.
21. G. Chiesa, A. Zajch, Geo-climatic applicability of earth-to-air heat exchangers in North America, Energy and Buildings. 202 (2019) 109332.
22. N. Artmann, H. Manz, P. Heiselberg, Climatic potential for passive cooling of buildings by night-time ventilation in Europe, Applied Energy. 84 (2007) 187–201. https://doi.org/10.1016/j.apenergy.2006.05.004.
23. EN 16798-1:2019, Energy performance of buildings. Ventilation for buildings. Indoor environmental input parameters for design and assessment of energy performance of buildings addressing indoor air quality, thermal environment, lighting and acoustics. Module M1-6, CEN, 2019.
24. G. Chiesa, Climatic potential maps of ventilative cooling techniques in Italian climates including resilience to climate changes, IOP Conf. Ser.: Mater. Sci. Eng. 609 (2019) 032039. https://doi.org/https://doi.org/10.1088/1757-899X/609/3/032039.
25. F. Allard, ed., Natural ventilation in buildings: a design handbook – EC, ALTENER Prorgamme, James and James (Science Publishers) Ltd, London, 1998.
26. P. Fanger, Thermal comfort-analysis and applications in environmental engineering. PhD, Technical University of Denmark, 1970.
27. J. van Hoof, Forty years of Fanger's model of thermal comfort: comfort for all?, Indoor Air. 18 (2008) 182–201. https://doi.org/10.1111/j.1600-0668.2007.00516.x.

28. EDYCE, D1.2 Operational dynamic Energy Perfomance Certificate (EPC) specifications, PoliTO, 2021. https://edyce.eu/reports-and-results/.
29. M.A. Humphreys, F. Nicol, S. Roaf, Adaptive thermal comfort: foundations and analysis., ROUTLEDGE, S.l., 2020.
30. F. Nicol, M. Humphreys, Derivation of the adaptive equations for thermal comfort in free-running buildings in European standard EN15251, Building and Environment. 45 (2010) 11–17. https://doi.org/10.1016/j.buildenv.2008.12.013.
31. M. Pellegrino, M. Simonetti, G. Chiesa, Reducing thermal discomfort and energy consumption of Indian residential buildings: Model validation by in-field measurements and simulation of low-cost interventions, Energy and Buildings. 113 (2016) 145–158. https://doi.org/10.1016/j.enbuild.2015.12.015.
32. E. Neufert, G.M. Di Giuda, V. Villa, A. Gottfried, P. Piantanida, Enciclopedia pratica per progettare e costruire: manuale a uso di progettisti, costruttori, docenti e studenti : fondamenti, norme e prescrizioni per progettare, costruire, dimensionare e distribuire a misura d'uomo, U. Hoepli, Milano, 2013.
33. B. Zevi, L. Zevi, C. Mancosu, Il nuovissimo manuale dell'architetto: [nozioni generali di progettazione, prestazioni degli organismi edilizi, esercizio professionale, progettazione ..., Mancosu, Roma, 2019.
34. G. Chiesa, M. Palme, Assessing climate change and urban heat island vulnerabilities in a built environment, TECHNE – Journal of Technology for Architecture and Environment. (2018) 237–245 Pages. https://doi.org/10.13128/TECHNE-22086.
35. DOE, NREL, EnergyPlus™, DOE, BTO, NREL, 2020. https://energyplus.net/.
36. Meteotest, METEONORM, METEOTEST Genossenschaft, Bern, 2015. meteonorm.com.
37. openpolis, GeoJSON, (2018). https://github.com/openpolis/geojson-italy.
38. ISTAT, Principali statistiche geografiche sui Comuni, (2021). https://www.istat.it/it/archivio/156224.
39. P. Heiselberg, Ventilative Cooling Principles, Potential and Barriers, in: Innovations in Ventilative Cooling, Springer International Publishing, Cham, 2021: p. 22. https://doi.org/10.1007/978-3-030-72385-9.
40. PRELUDE, PRELUDE (prescient building operation utilizing real time data for energy dynamic optimisation) project, (2021). https://prelude-project.eu/.

Giacomo Chiesa Giacomo Chiesa is an associate professor in Architectural Technology at Politecnico di Torino, Department of Architecture and Design. He holds a PhD in Technological Innovation for the Built Environment. His research focuses on bioclimatic and climatic design, passive solutions for heating and cooling buildings, ICT and IT integration in the urban and architectural contexts, intelligent buildings, and smart cities. He leads a research group that pursues a performance-driven methodological approach for design and operative optimisation/management issues correlated to the built environment at the different scales (components, buildings, urban contexts). He is a member of the POLITO's Didactical Board in Architecture and the Didactical Board in Electronic, Telecommunication and Physics Engineering. He is currently the local PI of two EU H2020 Innovation Action-funded projects and, during his 15 years of career, has authored more than 120 scientific publications.

Francesca Fasano Francesca Fasano holds a bachelor's degree in Physical Engineering and a master's degree with Laude in Telecommunication Engineering (ICT for Smart Society) at Politecnico di Torino; she is currently a research fellow at POLITO, Department of Architecture and Design, supporting ICT and IT integrated issues for the built environment. Additionally, to python coding and tool development actions, she keeps building energy management and optimisation, building monitoring and advanced building simulation, including climate and climate change analyses.

Paolo Grasso Paolo Grasso holds a bachelor's degree in Telecommunication Engineering and a master's degree in Telecommunication Engineering (ICT for Smart Society) at Politecnico di Torino. He is a research fellow at the same university at the Department of Architecture and Design. He supports python coding, forecasting building behaviours, and building energy monitoring and management. He works in the ICT and IoT integration in building stocks, including IT platform development and server facility management.